Selective Golgi export of Kir2.1 controls the stoichiometry of functional Kir2.x channel heteromers

Alexis Hofherr, Bernd Fakler and Nikolaj Klöcker*

Department of Physiology II, University of Freiburg, Hermann-Herder-Str. 7, 79104 Freiburg, Germany

*Author for correspondence (e-mail: nikolaj.kloecker@physiologie.uni-freiburg.de)

Journal of Cell Science

Summary

Surface expression of ion channels and receptors often depends on intrinsic sequence motifs that control their intracellular transport along the secretory pathway. Although members of the Kir2.x subfamily share two such motifs – a diacidic ER export motif and a positively charged Golgi export motif – they strongly differ in their surface expression. Whereas Kir2.1 shows prominent plasma membrane localization, Kir2.4 channels accumulate within the Golgi complex. By constructing chimeras between Kir2.1 and Kir2.4 subunits, a stretch of 20 amino acids was identified in the Kir2.1 C-terminus that is both necessary and sufficient to promote anterograde transport of Kir channel subunits at the level of trafficking from the Golgi to the plasma membrane. The core element of the identified sequence bears a tyrosine-dependent $Y XX\Phi$ consensus motif for adaptin binding, with the flanking residues determining its functional efficiency. As the signal is dominant in promoting surface transport of Kir2.1/Kir2.4 channel heteromers and is recognized by both the epithelial and neuronal intracellular sorting machinery, the preferential Golgi export of Kir2.1 will control the stoichiometry of Kir2.x heteromers expressed on the cell surface.

Introduction

Inwardly rectifying potassium (Kir) channels exert diverse cellular functions, such as controlling membrane excitability, heart rate, hormone release and neuronal signal transduction (Hille, 1992). Seven subfamilies of Kir channels have been identified based on sequence similarity and functional properties (Doupnik et al., 1995; Fakler and Ruppersberg, 1996; Nichols and Lopatin, 1997; Krapivinsky et al., 1998; Döring et al., 1998). Members of the Kir2.x subfamily share the biophysical characteristic of strong inward rectification that is due to a highly voltage-dependent block of the channel pore by intracellular polyamines and Mg^{2+} (Lopatin et al., 1994; Fakler et al., 1995). Voltage-dependent inward rectification enables Kir2.x channels to stabilize the resting membrane potential near the K^+ equilibrium potential and prevents them from shunting action potentials. The four members of the Kir2.x subfamily (Kir2.1-2.4) are expressed in both overlapping and differential patterns in brain, heart, skeletal muscle and endothelial cells (Nichols and Lopatin, 1997; Töpert et al., 1998). The expression patterns and the functional diversity of native inward-rectifier K^+ currents suggest that channels may form heteromers. Indeed, a recent study has conclusively demonstrated that Kir2.1 can co-assemble with all other members of its subfamily (Preisig-Müller et al., 2002). Therefore, mutations in Kir2.1 may impair the function of both homomeric Kir2.1 and heteromeric channels formed with other Kir2.x subunits. Heteromultimerization may in fact contribute to the heterogeneous phenotype of Andersen's syndrome, a

Kir2.1 channelopathy with cardiac arrhythmias, periodic paralysis and developmental dysmorphisms (Plaster et al., 2001; Jongsma and Wilders, 2001).

Cellular excitability is not only determined by the type of ion channels but also by the number present in the plasma membrane. Surface expression of ion channels and other integral membrane proteins might be controlled beyond the level of protein biosynthesis by intrinsic signal motifs that promote anterograde or retrograde transport along the secretory pathway (Griffith, 2001; Ma and Jan, 2002). These sequence motifs work by recruiting specific coat protein complexes that induce the formation of transport vesicles not only destined for certain subcellular localizations but also preferentially loaded with the respective cargo protein (Bonifacino and Lippincott-Schwartz, 2003). Whereas biochemical and structural work has shed light on the molecular mechanisms of selective transport along the early secretory pathway (Bonifacino and Glick, 2004; Lee et al., 2004), the mechanisms of transport from the Golgi to the plasma membrane are far less understood. We and others have recently identified two anterograde trafficking signals in Kir2.1 channels that control surface expression of the channel by promoting its export from the endoplasmic reticulum (ER) and from the Golgi complex (Ma et al., 2001; Stockklausner et al., 2001; Stockklausner and Klöcker, 2003). Despite both sequence motifs being highly conserved among all members of the Kir2.x subfamily, their plasma membrane expression differs strongly. In the present study, we have characterized an

anterograde trafficking signal in Kir2.1 that is both necessary for efficient transport of the channel to the cell surface and sufficient to increase surface transport of Kir2.4 at the level of Golgi-to-plasma membrane traffic. Since it also controls surface expression of heteromeric Kir2.1/Kir2.4 complexes, we propose that the motif governs the stoichiometry of functional Kir2.x channel heteromers.

Materials and Methods
Gene construction
N-terminal fusion constructs of Kir channel subunits with enhanced green fluorescent protein (EGFP) were designed by inserting the respective cDNA in-frame into the EGFP-C1 eukaryotic expression plasmid (BD Biosciences). Mutagenesis was done as described elsewhere (Stockklausner et al., 2001) and verified by sequencing. The hemagglutinin (HA) epitope was introduced into the extracellular domains of mKir2.1 and gpKir2.4 at amino acid positions 116 and 122, respectively. A dominant-negative dynamin-1 mutant (K44A) was kindly provided by S. L. Schmid (Scripps Institute, La Jolla, CA).

Cell culture and transfection
Opossum kidney (OK) cells (American Type Culture Collection) were grown in DMEM-F12 supplemented with 10% fetal calf serum (FCS) and 1% penicillin/streptomycin (P/S; Invitrogen) at 37°C in 5% CO_2. COS-7 cells and tsA201 cells (kindly provided by P. Dallos, Northwestern University, Evanston, IL) were grown at the same conditions in DMEM supplemented with 10% FCS and 1% P/S (Invitrogen). At ~80% confluence, cells were transfected with the respective cDNAs using Effectene Reagent (Qiagen) following the supplier's directions. The Golgi complex was identified by expressing a fusion construct consisting of the 81 N-terminal amino acids of the Golgi-resident enzyme 1,4-galactosyltransferase and red fluorescent protein DsRed2 (Stockklausner and Klöcker, 2003). In addition, cells were incubated with 10 µg/ml brefeldin A (BFA; Sigma-Aldrich), which reversibly fuses the Golgi compartment with the ER.

Primary cultures of hippocampal neurons were obtained from rats at P0. The entire hippocampus was isolated and dissociated with papain, and cells were plated in a 24-well plate at a density of ~80,000 cells/well in Neurobasal medium (Invitrogen) supplemented with B27, L-Glutamine and 1% P/S. Hippocampal neurons were grown at 37°C in 5% CO_2 on coverslips coated with poly-D-lysine and collagen (Invitrogen). They were transfected on DIV7 with Lipofectamine 2000 (Invitrogen) according to the manufacturer's recommendations, except that 1.2 µg of each cDNA in 25 µl Opti-MEM and 0.7 µl of Lipofectamine 2000 in 25 µl Opti-MEM were mixed and added to coverslips. Two days after transfection, cells were processed for surface immunocytochemistry as described below.

Immunocytochemistry
For immunocytochemical detection of the HA epitope, transfected cells were fixed in 4% paraformaldehyde in phosphate-buffered saline (PBS) for 15 minutes at 4°C and pretreated with 10% normal goat serum (NGS) in PBS with 0.05% Triton X-100 (PBS-T) for 1 hour at room temperature (RT) to block unspecific antibody binding. Then they were incubated with a monoclonal mouse anti-HA antibody (Santa Cruz Biotechnology) diluted 1:200 in 2% NGS/PBS-T for 1 hour at RT. Immunoreactivity was visualized by a goat anti-mouse IgG secondary antibody conjugated to cy-3 (1:1000 in 10% NGS/PBS-T). To detect selectively the population of HA-tagged channels expressed on the cell surface or for endocytosis assays, antibody staining was performed in vivo without use of detergents. Unless otherwise stated, antibody incubation was carried out before fixation in serum-free medium for 15 minutes at 37°C for the primary

and secondary antiserum, respectively. The in vivo labeling approach often led to a clustered surface distribution of the respective constructs that was artificially induced by antibody crosslinking (Delling et al., 2002).

Immunoblot analysis
36 hours after transfection, cells were lysed in TEEN-T (50 mM Tris pH 7.6, 1 mM EDTA, 1 mM EGTA, 150 mM NaCl, 1% Triton X-100, protease inhibitors) for 30 minutes on ice. Nuclei and cell debris were pelleted by low-speed centrifugation at 1000 g for 5 minutes at 4°C. The supernatants were separated by reducing SDS-PAGE on a 10% polyacrylamide gel, transferred onto PVDF membranes and incubated with a mouse monoclonal anti-GFP antibody (1:5000; BD Biosciences). Following incubation with a secondary HRP-conjugated anti-mouse IgG antiserum (1:2500; Santa Cruz Biotechnology), labeled proteins were detected using ECL-plus reagent (Amersham Biosciences). Density analysis of labeled protein bands was carried out using Scion Image 4.02.

Quantification of surface expression
All mutant Kir channels were tagged with an extracellular HA epitope and surface expression was quantified by fluorescence intensity measurements of anti-HA immunocytochemistry without use of detergents, as described before (Stockklausner and Klöcker, 2003). To exclude differences in antibody binding affinities, only surface expression levels of constructs with the same extracellular domain structure were compared with each other (Kir2.1 versus intracellular Kir2.1 mutants or Kir2.4 versus intracellular Kir2.4 mutants, respectively). For each construct, pixel intensity values of stainings from at least two independent transfections were corrected for background and integrated over 10 areas of 0.2116 mm^2 each (Scion Image 4.02). Wild-type (control) and mutant (test) constructs were always processed in parallel. Surface fluorescence intensity values were related to the translation efficiencies of the respective constructs determined by immunoblot analysis. We preferred immunoblot analysis to determine total protein levels over an approach employing GFP fluorescence intensity, because several channel constructs accumulated in the Golgi complex leading to local saturation of the GFP fluorescence signal when imaging all subcellular regions of a given cell. Statistically significant differences were assessed using the unpaired Student's t-test. Data are given as mean±s.e.m. expressed as relative surface expression levels of the respective control.

Imaging
Cells were imaged with a confocal laser scanning microscope (LSM510, Zeiss) using the following excitation wavelengths and filter settings: EGFP, excitation 488 nm Ar laser/emission BP505-530 nm; cy-3, excitation 543 nm He laser/emission LP560 nm.

Results
Kir2.1 and Kir2.4 differ in their degree of surface expression
When heterologously expressed in opossum kidney (OK) cells, the inward-rectifier K^+ channels Kir2.1 and Kir2.4 exhibit different levels of cell-surface expression (Fig. 1A). Thus, GFP-fused Kir2.1 ($_{GFP}$Kir2.1) was predominantly found in the Golgi complex and the plasma membrane (Stockklausner et al., 2001), whereas GFP-fused Kir2.4 ($_{GFP}$Kir2.4) was predominantly concentrated in a juxtanuclear compartment. As judged from plasma membrane fluorescence, the amount of $_{GFP}$Kir2.4 present on the cell surface was significantly lower
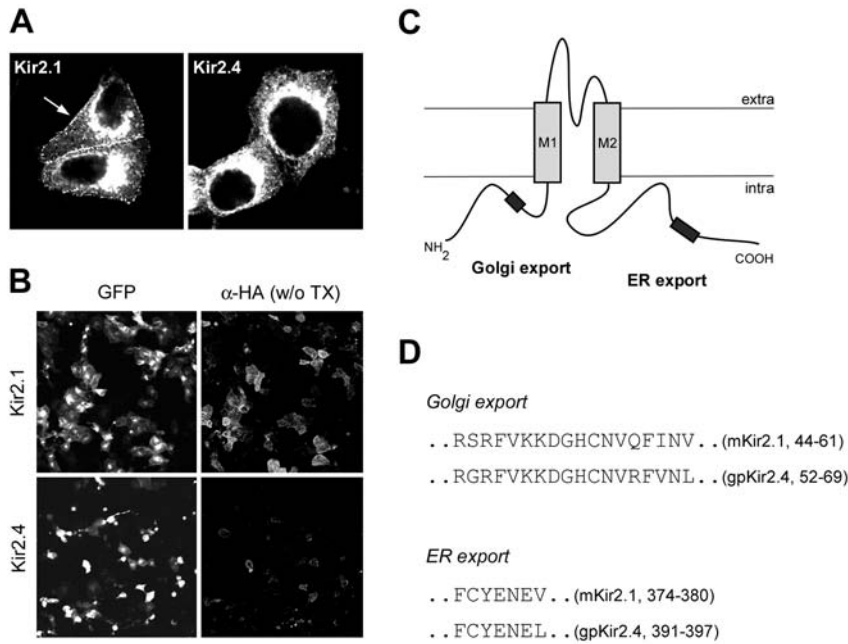
Fig. 1. Kir2.1 and Kir2.4 show different levels of surface expression. (A) Representative confocal images of OK cells expressing ₍GFP₎Kir2.1 and ₍GFP₎Kir2.4. Note that only ₍GFP₎Kir2.1 shows distinct plasma membrane fluorescence (arrow). (B) Surface expression of extracellularly HA-tagged ₍GFP₎Kir2.1 and ₍GFP₎Kir2.4 detected by α-HA immunocytochemistry without membrane permeabilization (TX, Triton X-100; see Materials and Methods). (C) Cartoon depicting the membrane topology of Kir channels. The cytoplasmic N- and C-terminal domains contain trafficking signals for efficient ER and Golgi export, respectively (Ma et al., 2001; Stockklausner et al., 2001; Stockklausner and Klöcker, 2003). (D) Sequence alignment of the known trafficking signals in Kir2.1 and Kir2.4.

than that of ₍GFP₎Kir2.1. The observation with GFP-fused Kir subunits was corroborated by experiments that selectively detected channel proteins in the plasma membrane by means of an extracellular epitope tag (Fig. 1B). These findings were somewhat surprising given that both Kir2 subunits contain the two previously identified anterograde trafficking signals (Fig. 1C,D), a diacidic sequence motif in the C-terminus promoting ER export (Ma et al., 2001; Stockklausner et al., 2001) and a positively charged cluster motif in the N-terminus conferring efficient Golgi export (Stockklausner and Klöcker, 2003). Consequently, there must exist further intrinsic sequence information controlling the subcellular distribution of these Kir channel subunits.

Golgi-to-plasma membrane transport of Kir2.4 is less efficient

First, we investigated the subcellular trafficking of ₍GFP₎Kir2.4 in more detail. As shown in Fig. 2A, ₍GFP₎Kir2.4 channels accumulated within the Golgi complex as indicated by colocalization with the red fluorescent protein DsRed fused to the targeting sequence of the Golgi-resident enzyme galactosyltransferase I and by reversible redistribution into the ER after incubation with the fungal Golgi toxin BFA. Either a slow anterograde Golgi-to-plasma membrane transport or a high rate of endocytosis and retrograde transport to the trans-Golgi network (TGN) could account for the accumulation of ₍GFP₎Kir2.4 protein in the Golgi complex. To distinguish between these alternatives, we performed surface labeling of ₍GFP₎Kir2.4 in vivo to detect retrograde transport of endocytosed ₍GFP₎Kir2.4 to the TGN (Fig. 2B). Cells expressing extracellularly HA-tagged ₍GFP₎Kir2.4 were incubated with α-HA antibody for different periods of time (3-16 hours) before labeled protein complexes were visualized by incubation with a fluorescent secondary antiserum after fixation and permeabilization of the cells. As antibody labeling could interfere with retrograde transport of the channel and lead to mistargeting into lysosomes, experiments were performed in the presence of the

membrane-permeable leupeptin analog ALLN (100 µM) to prevent degradation of internalized antibody in lysosomes. No accumulation of α-HA immunoreactivity was observed within the Golgi complex or within any other intracellular compartment even after 16 hours. Only weak plasma membrane staining was seen, indicating no substantial internalization within 16 hours. In good agreement with these data, inhibition of clathrin-dependent endocytosis by co-expressing a dominant-negative dynamin-1 mutant (dn-Dyn) (Damke et al., 1994) did not change the subcellular distribution of ₍GFP₎Kir2.4 (Fig. 2B), whereas endocytic transferrin uptake was inhibited (Fig. S1 in supplementary material). These results strongly suggest that the different levels of surface expression of ₍GFP₎Kir2.1 and ₍GFP₎Kir2.4 are due to less efficient anterograde transport of ₍GFP₎Kir2.4 to the plasma membrane.

Sequence information in the Kir2.1 C-terminus is both necessary and sufficient for efficient surface targeting

To identify the difference in sequence responsible for the distinct trafficking patterns, we designed chimeras of Kir2.1 and Kir2.4 by swapping their cytoplasmic N- and C-terminal domains (Fig. 3A). In a first set of experiments, the C-terminal domain of Kir2.1 was found to contain the critical targeting information for efficient plasma membrane expression (Fig. 3B). A more detailed analysis of the surface expression of further C-terminal chimeras revealed that a stretch of 20 amino acids within the Kir2.1 C-terminus was necessary for efficient plasma membrane targeting and was sufficient to increase surface expression of ₍GFP₎Kir2.4 by approximately 4-fold (Fig. 3C,D). These findings were independent of the epithelial cell type used; similar results were obtained in COS-7 cells [₍GFP₎Kir2.4, 1±0.33; ₍GFP₎Kir2.4-int(2.1), 4.19±0.7; $P<0.01$].

The experiments described so far do not distinguish between a forward trafficking signal in Kir2.1 that actively promotes anterograde Golgi-to-plasma membrane transport or a Golgi retention signal in Kir2.4 that might have been abolished in the C-terminal ₍GFP₎Kir2.4/Kir2.1 chimeras. We therefore
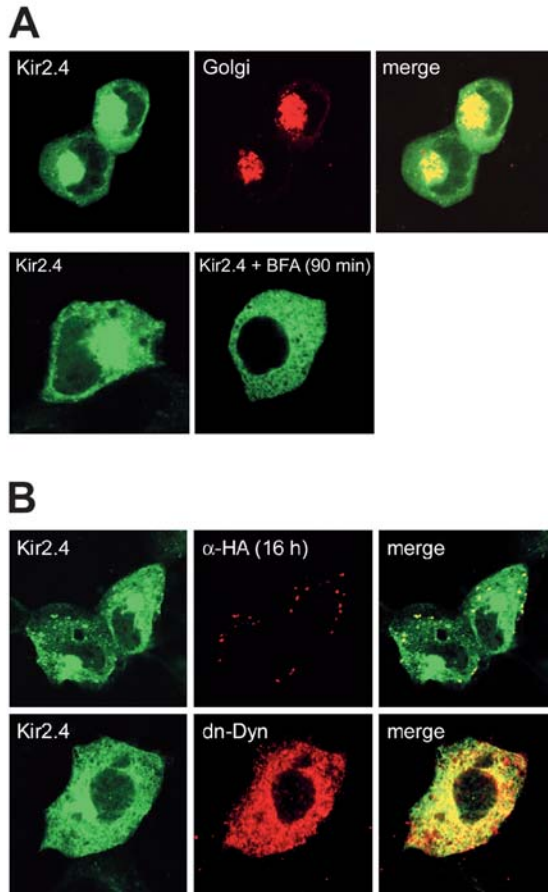
Fig. 2. Kir2.4 accumulates in the Golgi complex. (A) Representative confocal images showing the subcellular distribution of $_{GFP}$Kir2.4 in OK cells. Golgi accumulation is shown by co-localization of $_{GFP}$Kir2.4 with DsRed2 fused to the targeting sequence of 1,4-galactosyltransferase (Golgi; upper panel) and redistribution of Kir2.4 into the ER by incubation with brefeldin A (BFA; lower panel). (B) Golgi accumulation of $_{GFP}$Kir2.4 is not due to retrograde transport to the Golgi complex. Extracellular epitope tagging does not reveal significant internalization of $_{GFP}$Kir2.4 after 16 hours (upper panel); inhibition of clathrin-dependent endocytosis by co-expression of a HA-tagged dominant-negative dynamin (dn-Dyn) mutant (dynamin-K44A) (Damke et al., 1994) does not affect the subcellular distribution of $_{GFP}$Kir2.4 (lower panel).

exchanged the identified stretch of amino acids for a flexible glycine/serine-linker ($_{GFP}$Kir2.1-GS, $_{GFP}$Kir2.4-GS). Whereas surface expression of $_{GFP}$Kir2.4 did not change after inserting the GS linker, surface expression of $_{GFP}$Kir2.1-GS was significantly reduced compared with the wild-type channel (Fig. 3E). These data argue in favor of an active forward trafficking signal in the Kir2.1 C-terminus.

The alignment of the identified C-terminal segments exhibits a high degree of sequence homology between the two channels with very few non-conservative residue exchanges (Fig. 4A). A central element of the sequence stretch consists of the residues YIPL, which closely resemble the consensus motif Y$XX\Phi$ known to confer binding to adaptins (with X for any amino acid and Φ for a bulky, hydrophobic residue). Mutation of all four amino acids to alanine (YIPL-AAAA) significantly reduced surface expression of Kir2.1, implicating this sequence

motif in the surface transport of the channel (Fig. 4B). Moreover, the sole exchange of the tyrosine residue for alanine (Y242A) was sufficient to decrease surface expression of Kir2.1. However, as this consensus motif is conserved between Kir2.1 and Kir2.4, it cannot explain the different rates in their Golgi-to-plasma membrane transport. We thus focused on residues surrounding the YIPL motif for further sequence characterization of the identified trafficking determinant (Fig. 4C). Homologous exchange of both proline residues P242 and P246 upstream of YIPL in the Kir2.4 C-terminal sequence for serine residues significantly increased surface expression compared with wild-type ($_{GFP}$Kir2.4-P242S,P246S). The increase in surface expression was even more evident if all residues upstream of the YIPL motif were adapted to the Kir2.1 sequence. Still, this mutation did not completely reproduce the effects of the whole 20 residue motif identified in the Kir2.1 C-terminus in promoting surface expression of Kir2.4 [$_{GFP}$Kir2.1-KSRITS, 2.6 ± 0.2; $_{GFP}$Kir2.4-int(2.1), 4.72 ± 0.5], which indicates that residues downstream of the YIPL motif must also be important for its efficiency.

Finally, we tested whether the function of the trafficking determinant depended upon its intramolecular position. Instead of inserting it at the homologous position, the stretch of 20 amino acids containing the Golgi-to-plasma membrane signal was fused to the very N- and C-termini of Kir2.4, respectively. Whereas the C-terminal fusion construct ($_{GFP}$Kir2.4-signal-C) was retained in the ER, the N-terminal fusion construct ($_{GFP}$Kir2.4-signal-N) was readily exported from the ER and reached the Golgi complex. However, surface expression of $_{GFP}$Kir2.4-signal-N was not increased over wild-type Kir2.4, suggesting that the sequence motif was non-functional at this position ($_{GFP}$Kir2.4, 1 ± 0.15; $_{GFP}$Kir2.4-signal-N, 1.16 ± 0.38; not significant).

The identified trafficking determinant controls surface transport of channel heteromers

Since Kir2.1 and Kir2.4 are able to form channel heteromers (Preisig-Müller et al., 2002; Schram et al., 2002), we addressed the question of whether the identified signal governs Golgi-to-plasma membrane traffic of heteromeric channels. Equal amounts of cDNAs coding for extracellularly HA-tagged Kir2.4 (Kir2.4-HA) were either expressed alone or co-expressed with $_{GFP}$Kir2.1 (without HA-tag) and surface expression of Kir2.4-HA was quantified. As shown in Fig. 5A, co-expression of $_{GFP}$Kir2.1 significantly increased the amount of Kir2.4-HA expressed on the cell surface. In a control experiment, we compared surface expression of Kir2.4-HA co-expressed either with $_{GFP}$Kir2.1 or with $_{GFP}$Kir2.1-int(2.4) lacking the identified trafficking determinant. Supporting a role for surface transport of channel heteromers, we observed that removing the critical sequence stretch from co-expressed Kir2.1 [$_{GFP}$Kir2.1-int(2.4)] led to a significant decrease in the amount of Kir2.4-HA on the cell surface when compared with the heteromeric assembly of wild-type $_{GFP}$Kir2.1 and Kir2.4-HA (Fig. 5B).

Recognition of the identified transport motif is conserved in neurons

As the recognition of trafficking signals might vary with cell
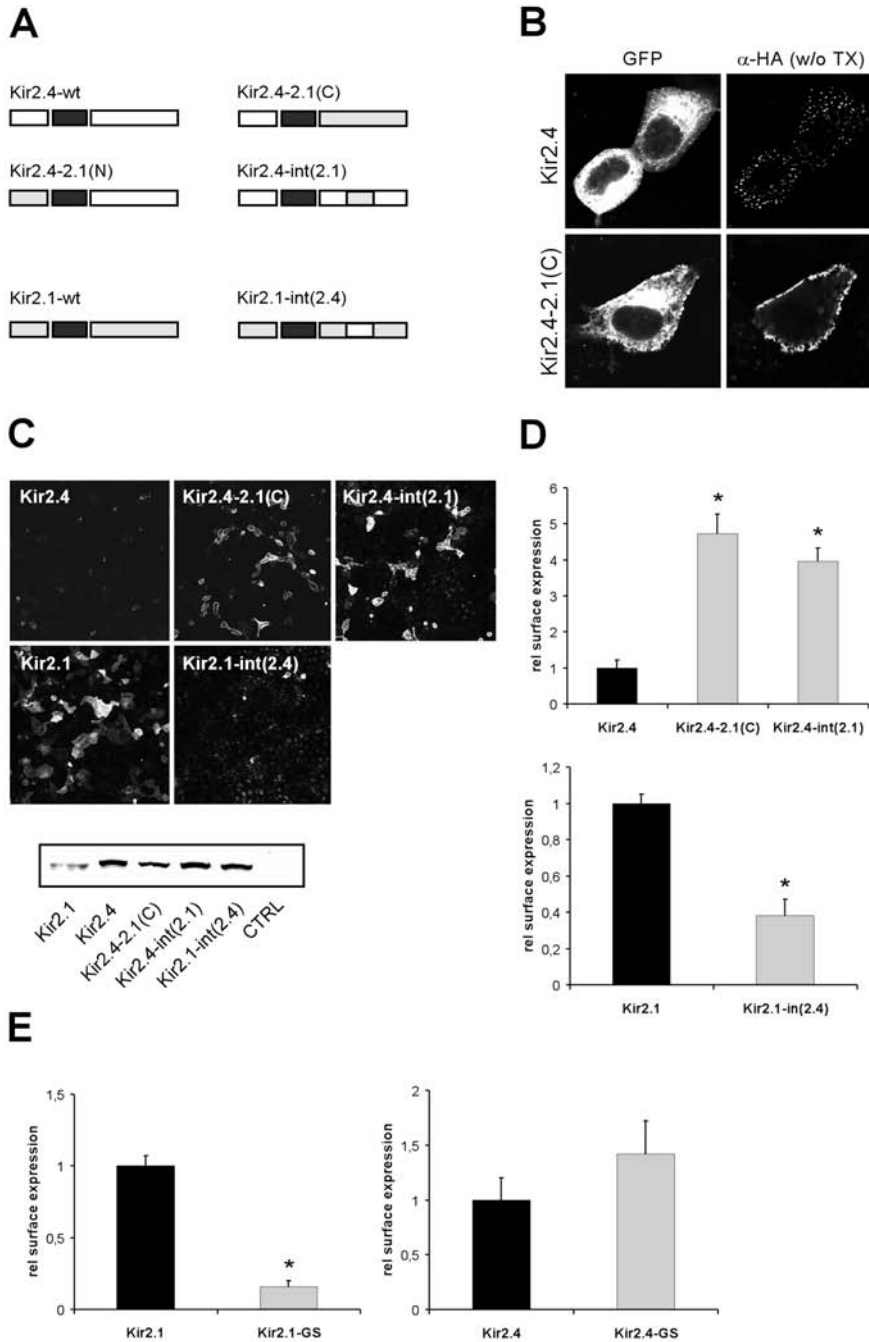
A

B

C

D

E

Fig. 3. Sequence information in the Kir2.1 C-terminus is both necessary and sufficient to promote Golgi-to- plasma membrane transport. (A) Schematic drawing of Kir2.1/Kir2.4 chimeric constructs. Kir2.4-2.1(N): $_{1-77}$Kir2.4 was substituted by $_{1-69}$Kir2.1; Kir2.4-2.1(C): $_{212-439}$Kir2.4 was substituted by $_{204-428}$Kir2.1; Kir2.4-int(2.1): $_{241-260}$Kir2.4 was replaced by $_{233-252}$Kir2.1; Kir2.1-int(2.4): $_{233-252}$Kir2.1 was replaced by $_{241-260}$Kir2.4. (B) The C-terminal domain of Kir2.1 contains critical sequence information that is sufficient to increase Kir2.4 surface expression. Representative confocal images of OK cells expressing extracellularly HA-tagged $_{GFP}$Kir2.4 and $_{GFP}$Kir2.4-2.1(C), processed for α-HA immunocytochemistry without membrane permeabilization (TX: Triton X-100). (C) A stretch of 20 amino acids of Kir2.1 ($_{233-252}$Kir2.1) is sufficient to increase surface expression of Kir2.4 and necessary for efficient surface expression of Kir2.1. Representative confocal images of OK cells expressing the indicated extracellularly HA-tagged constructs, processed for detecting their surface expression. Total protein expression of the various constructs is similar as shown in α-GFP immunoblot analysis below. (D) Quantification of the surface expression experiments in (C). (E) The Kir2.1 trafficking determinant actively promotes Golgi-to-plasma membrane transport. Substitution of $_{233-252}$Kir2.1 by a flexible glycine-serine linker peptide (Kir2.1-GS) reduces surface expression of Kir2.1, whereas Kir2.4 surface expression remains unaffected by homologous substitution of $_{241-260}$Kir2.4 by the linker peptide (Kir2.4-GS). *Statistically significant when compared with respective controls ($P<0.01$; unpaired Student's t-test; see Materials and Methods).

type and native co-expression of Kir2.1 and Kir2.4 is restricted to neurons (Töpert et al., 1998), we tested whether the identified trafficking determinant promotes surface transport of Kir channels in neurons. Primary hippocampal cultures were transfected with extracellularly HA-tagged $_{GFP}$Kir2.4 and $_{GFP}$Kir2.4-int(2.1), respectively, and processed for anti-HA immunocytochemistry without membrane permeabilization. Similar to what had been observed in epithelial cells, the identified signal motif was sufficient to increase surface expression of Kir2.4 significantly, by a factor of ~4. This indicates that the identified trafficking motif participates in a general sorting mechanism conserved across cell types (Fig. 6).

Discussion

Here, we characterized an anterograde trafficking motif in the cytoplasmic C-terminus of Kir2.1 channels that is not only necessary to promote its Golgi-to-plasma membrane transport in both epithelial cells and neurons, but is also sufficient to increase surface expression of Kir2.4 when inserted at the homologous position. As it also controls surface transport of heteromeric Kir2.1/Kir2.4 channels, we propose that the identified motif governs the stoichiometry of Kir2.x heteromers on the cell surface.

The transport of cargo protein between the various intracellular compartments of the secretory pathway is accomplished by transport carriers that form at sites at which
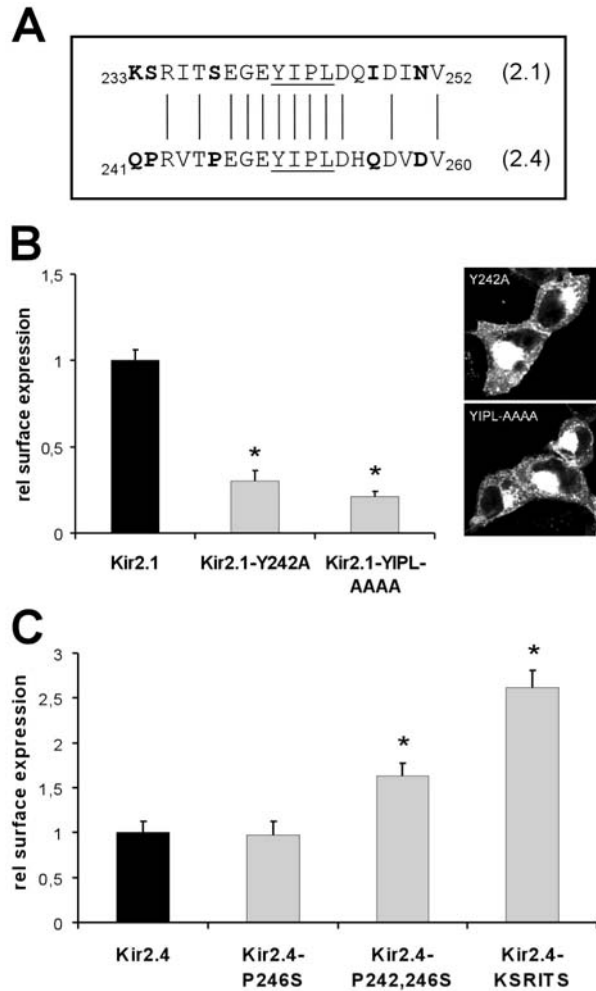
Fig. 4. Sequence characterization of the Golgi-to-plasma membrane trafficking determinant in Kir2.1. (A) Primary sequence alignment of the identified trafficking determinant in Kir2.1 with the homologous sequence of Kir2.4. Non-conservative exchanges are in bold letters, the Y$XX\Phi$ consensus motif for adaptin binding is underlined. (B,C) Quantification of surface expression of Kir2.1 mutants and Kir2.4 mutants as indicated. Note that the Kir2.1 mutants in (B) show Golgi accumulation, indicating that the decrease in surface expression is not due to folding or ER export defects but to impaired post-Golgi transport. *Statistically significant when compared with respective controls ($P<0.01$; unpaired Student's t-test; see Materials and Methods).

Fig. 5. The Kir2.1 Golgi-to-plasma membrane trafficking signal governs surface expression of Kir2.1/Kir2.4 heteromers. (A) Co-expression of GFPKir2.1 increases surface expression of HA-tagged Kir2.4. (B) Co-expression of Kir2.1 with the identified trafficking signal having been replaced by the homologous Kir2.4 sequence [Kir2.1-int(2.4)] reverses the effects of co-expressed wild-type GFPKir2.1 on promoting surface expression of HA-tagged Kir2.4. *Statistically significant when compared with respective control ($P<0.01$; unpaired Student's t-test; see Materials and Methods).

compartment-specific coat protein complexes have been recruited. These coat proteins not only participate in the formation of coated vesicular carriers, but also confer cargo selection by interacting with specific sorting signals contained in the cytoplasmic domains of cargo proteins (Bonifacino and Traub, 2003; Bonifacino and Lippincott-Schwartz, 2003). Mapping the identified Golgi-to-plasma membrane sorting signal onto the crystal structures of the bacterial K+ inward-rectifier channel KirBac1.1 or the eukaryotic G-protein-gated Kir3.1 subunit (Nishida and MacKinnon, 2002; Kuo et al., 2003), we assume an intramolecular position exposed to the cytoplasm. Such accessibility of the trafficking determinant from the cytoplasm is consistent with it serving as a recognition domain for coat protein complexes. Which coat protein
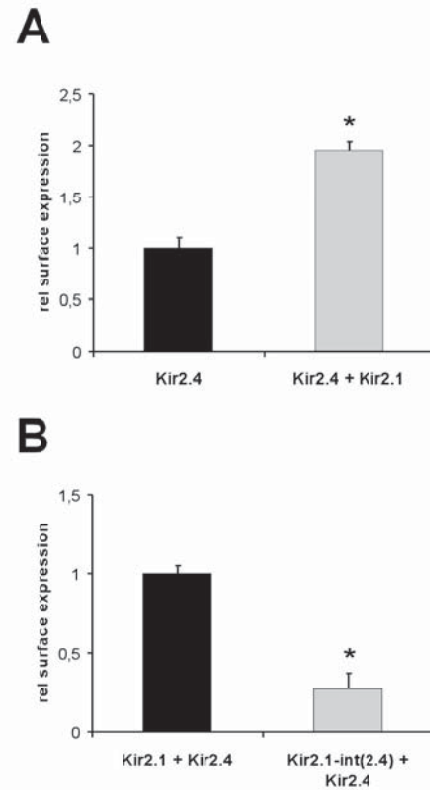
complexes should be considered as potential interaction partners, being able to bind to the Kir2.1 C-terminal sequence but failing to do so in Kir2.4? The signal sequence bears the motif YIPL, which closely resembles the consensus sequence Y$XX\Phi$ known to interact with adaptor protein (AP) complexes (Bonifacino and Traub, 2003). These are involved in vesicle formation for selective protein transport between different intracellular compartments: the AP-2 complex mediates rapid endocytosis from the plasma membrane; AP-1, AP-3 and AP-4 mediate sorting steps at the trans-Golgi network (TGN) and/or endosomes (Boehm and Bonifacino, 2001; Robinson and Bonifacino, 2001). Each of these complexes is composed of four adaptin subunits. In most cases, recognition of the Y$XX\Phi$ motif relies on the medium (μ) chain adaptin, but exceptions from this rule have been described (Ohno et al., 1995; Ohno et al., 1996; Hirst et al., 1999; Nishimura et al., 2002). Both functional and structural work shows that the tyrosine and hydrophobic Φ residue are essential for adaptin binding, whereas the X residues and sequence information flanking the tetrapeptide contribute to the affinity and specificity of AP binding (Ohno et al., 1995; Boll et al., 1996; Owen and Evans, 1998; Owen et al., 2001). Phosphorylation of the critical tyrosine residue has been shown to prevent

adaptin binding both in vitro and vivo (Boll et al., 1996; Ohno et al., 1996; Schaefer et al., 2002). In line with the hypothesis that the identified trafficking determinant serves as a recognition domain for an AP complex, we observed that not only mutation of YIPL to alanine but also the sole exchange of the tyrosine residue was sufficient to reduce surface expression of Kir2.1 significantly. Moreover, as YIPL is conserved between the two channels, we found the flanking residues upstream of YIPL to be crucial for explaining the different efficiencies between surface transport rates of Kir2.1 and Kir2.4. Until now, only the AP-1B, AP-3 and AP-4 complexes have been assigned a function in Golgi-to-plasma membrane traffic (Fölsch et al., 2001; Gan et al., 2002; Nishimura et al., 2002; Simmen et al., 2002). AP-1B and AP-4 are rather unlikely to be the interacting coats of the identified signal, because μ1B, the $Y XX\Phi$-recognizing subunit of the AP-1B complex, is exclusively expressed in polarized epithelia, whereas we found that the newly identified signal is functional across cell types; moreover, binding of μ4, the $Y XX\Phi$-recognizing

Fig. 6. The identified Golgi-to-plasma membrane trafficking motif is recognized by the neuronal sorting machinery. (A) Representative confocal images of hippocampal neurons expressing extracellularly HA-tagged $_{GFP}$Kir2.4 and $_{GFP}$Kir2.4-int(2.1), respectively. Surface expression of channel constructs was determined by α-HA immunocytochemistry without membrane permeabilization (TX, Triton X-100). The clustered distribution of $_{GFP}$Kir2.4-int(2.1) is artificially induced by the in vivo surface-labeling procedure. (B) Quantification of surface expression (n=10 neurons). Cy-3 fluorescence intensity values of neuronal surface stainings were corrected for background and related to total protein expression measured by GFP fluorescence. Data are given as relative intensity values per μm^2. *Statistically significant when compared with respective control (P<0.01; unpaired Student's t-test; see Materials and Methods).

subunit of AP-4, shows a preference for aromatic residues near the critical tyrosine, which are not found in Kir2.1 (Ohno et al., 1999; Aguilar et al., 2001). The AP-3 complex is mainly involved in transport between the TGN and lysosome-related organelles (Robinson and Bonifacino, 2001), but has also been implicated in surface transport of the vesicular stomatitis virus glycoprotein VSV-G (Nishimura et al., 2002). Signal recognition by AP-3 depends on acidic residues in the proximity of the critical tyrosine, and the signal-binding affinity of μ3A is regulated by upstream CK2 phosphorylation (Ohno et al., 1998; Madrid et al., 2001). Although the signal identified in Kir2.1 shares both of these sequence characteristics, preliminary experiments did not show the recruitment of μ3A to sites of Kir2.1 expression, which would indicate an interaction of the two proteins. In addition, the surface transport of Kir2.1 was not affected upon co-expression of a dominant-negative δ adaptin that had previously been shown to interfere with the AP-3-dependent VSV-G traffic to the cell surface (our unpublished work) (Nishimura et al., 2002).

Besides primary sequence characteristics, the intramolecular position of sorting signals with respect to their spatial distance from the plasma membrane can be critical for their recognition by coat protein complexes (Bonifacino and Traub, 2003; Shikano and Li, 2003). To test for a positional dependence, the signal identified in Kir2.1 was not only inserted at the homologous position into the Kir2.4 C-terminus but was also fused to its very N- and C-terminal ends, assuming this would increase the signal-to-membrane distance without limiting the accessibility of the signal. Indeed, increasing linear spacing of the signal with respect to the closest transmembrane domain of the channel resulted in a loss of its function. It has been shown
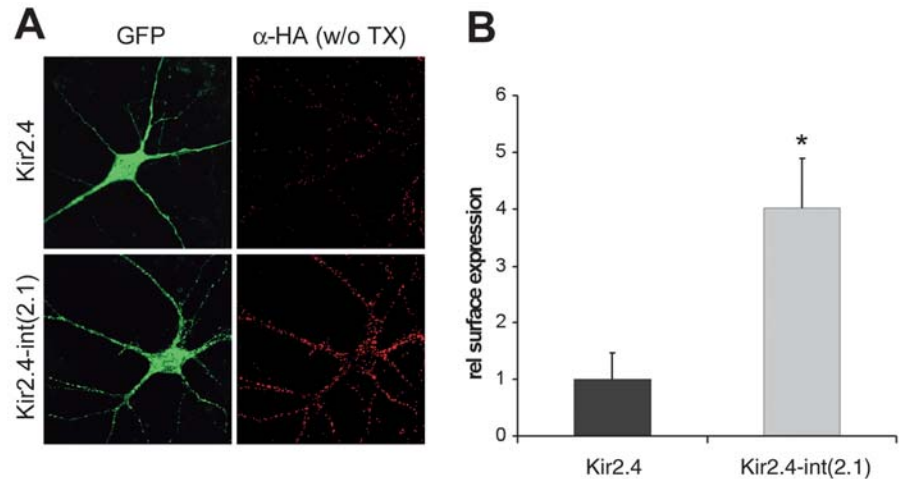
that components of various coat protein complexes, including AP complexes, can interact with phospholipids in the plasma membrane, which enhances signal recognition (Gaidarov et al., 1996; Collins et al., 2002; Rohde et al., 2002). Positional dependence of signal recognition could thus reflect the need for stabilizing plasma membrane interactions of the signal–coat-protein complex. This view is supported by a previous study demonstrating an important role of positively charged amino acids for selective Golgi export of Kir channels (Stockklausner and Klöcker, 2003). By electrostatic interaction, these positive charges could increase the local concentration of phosphoinositides in the vicinity of the channel and thereby favor the formation of a stable signal–coat-protein complex for its Golgi-to-plasma membrane traffic.

An alignment of the respective C-terminal segments shows complete conservation of the $Y XX\Phi$ motif between all members of the Kir2.x subfamily. However, the flanking residues differ; strikingly, serine 234 in Kir2.1 is replaced by proline in all other Kir2.x subunits. Since our experiments predict this residue to be critical for signal function, with a serine at this position promoting signal recognition and a proline preventing it, we propose Kir2.1 to be preferentially transported to the cell surface not only over Kir2.4 as shown here, but over all other members of its subfamily as well. What are the functional consequences of such differential trafficking? Assuming free assembly of channel heteromers at the level of the ER, our study suggests that Kir2.1 will govern the stoichiometry of functional Kir2.x heteromers (i.e. the heteromers expressed on the cell surface) by controlling the efficiency of their Golgi export. As demonstrated in the study, plasma membrane expression of Kir2.1 homomers and Kir2.1-

containing heteromers is preferred over surface expression of homomeric Kir2.4. Though the definite physiological consequences of this bias in surface stoichiometry of Kir2.x channels towards Kir2.1 subunits must remain speculative at this point, the present data further elucidate the dominant-negative effects of Kir2.1 mutations on Kir2.x currents, as seen in Andersen's syndrome.

References

Aguilar, R. C., Boehm, M., Gorshkova, I., Crouch, R. J., Tomita, K., Saito, T., Ohno, H. and Bonifacino, J. S. (2001). Signal-binding specificity of the mu4 subunit of the adaptor protein complex AP-4. *J. Biol. Chem.* **276**, 13145-13152.

Boehm, M. and Bonifacino, J. S. (2001). Adaptins: the final recount. *Mol. Biol. Cell* **12**, 2907-2920.

Boll, W., Ohno, H., Songyang, Z., Rapoport, I., Cantley, L. C., Bonifacino, J. S. and Kirchhausen, T. (1996). Sequence requirements for the recognition of tyrosine-based endocytic signals by clathrin AP-2 complexes. *EMBO J.* **15**, 5789-5795.

Bonifacino, J. S. and Glick, B. S. (2004). The mechanisms of vesicle budding and fusion. *Cell* **116**, 153-166.

Bonifacino, J. S. and Lippincott-Schwartz, J. (2003). Coat proteins: shaping membrane transport. *Nat. Rev. Mol. Cell. Biol.* **4**, 409-414.

Bonifacino, J. S. and Traub, L. M. (2003). Signals for sorting of transmembrane proteins to endosomes and lysosomes. *Annu. Rev. Biochem.* **72**, 395-447.

Collins, B. M., McCoy, A. J., Kent, H. M., Evans, P. R. and Owen, D. J. (2002). Molecular architecture and functional model of the endocytic AP2 complex. *Cell* **109**, 523-535.

Damke, H., Baba, T., Warnock, D. E. and Schmid, S. L. (1994). Induction of mutant dynamin specifically blocks endocytic coated vesicle formation. *J. Cell Biol.* **127**, 915-934.

Delling, M., Wischmeyer, E., Dityatev, A., Sytnyk, V., Veh, R. W., Karschin, A. and Schachner, M. (2002). The neural cell adhesion molecule regulates cell-surface delivery of G-protein-activated inwardly rectifying potassium channels via lipid rafts. *J. Neurosci.* **22**, 7154-7164.

Döring, F., Derst, C., Wischmeyer, E., Karschin, C., Schneggenburger, R., Daut, J. and Karschin, A. (1998). The epithelial inward rectifier channel Kir7.1 displays unusual K$^+$ permeation properties. *J. Neurosci.* **18**, 8625-8636.

Doupnik, C. A., Davidson, N. and Lester, H. A. (1995). The inward rectifier potassium channel family. *Curr. Opin. Neurobiol.* **5**, 268-277.

Fakler, B. and Ruppersberg, J. P. (1996). Functional and molecular diversity classifies the family of inward-rectifier K$^+$ channels. *Cell. Physiol. Biochem.* **6**, 195-209.

Fakler, B., Brändle, U., Glowatzki, E., Weidemann, S., Zenner, H. P. and Ruppersberg, J. P. (1995). Strong voltage-dependent inward rectification of inward rectifier K$^+$ channels is caused by intracellular spermine. *Cell* **80**, 149-154.

Fölsch, H., Pypaert, M., Schu, P. and Mellman, I. (2001). Distribution and function of AP-1 clathrin adaptor complexes in polarized epithelial cells. *J. Cell Biol.* **152**, 595-606.

Gaidarov, I., Chen, Q., Falck, J. R., Reddy, K. K. and Keen, J. H. (1996). A functional phosphatidylinositol 3,4,5-trisphosphate/phosphoinositide binding domain in the clathrin adaptor AP-2 alpha subunit. Implications for the endocytic pathway. *J. Biol. Chem.* **271**, 20922-20929.

Gan, Y., McGraw, T. E. and Rodriguez-Boulan, E. (2002). The epithelial-specific adaptor AP1B mediates post-endocytic recycling to the basolateral membrane. *Nat. Cell Biol.* **4**, 605-609.

Griffith, L. C. (2001). Potassium channels: the importance of transport signals. *Curr. Biol.* **11**, R226-R228.

Hille, B. (1992). *Ionic Channels of Excitable Membranes*, 2nd edn. Sunderland, MA: Sinauer Associates.

Hirst, J., Bright, N. A., Rous, B. and Robinson, M. S. (1999). Characterization of a fourth adaptor-related protein complex. *Mol. Biol. Cell* **10**, 2787-2802.

Jongsma, H. J. and Wilders, R. (2001). Channelopathies: Kir2.1 mutations jeopardize many cell functions. *Curr. Biol.* **11**, R747-R750.

Krapivinsky, G., Medina, I., Eng, L., Krapivinsky, L., Yang, Y. and Clapham, D. E. (1998). A novel inward rectifier K$^+$ channel with unique pore properties. *Neuron* **20**, 995-1005.

Kuo, A., Gulbis, J. M., Antcliff, J. F., Rahman, T., Lowe, E. D., Zimmer, J., Cuthbertson, J., Ashcroft, F. M., Ezaki, T. and Doyle, D. A. (2003). Crystal structure of the potassium channel KirBac1.1 in the closed state. *Science* **300**, 1922-1926.

Lee, M. C., Miller, E. A., Goldberg, J., Orci, L. and Schekman, R. (2004). Bi-directional protein transport between the ER and Golgi. *Annu. Rev. Cell Dev. Biol.* **20**, 87-213.

Lopatin, A. N., Makhina, E. N. and Nichols, C. G. (1994). Potassium channel block by cytoplasmic polyamines as the mechanism of intrinsic rectification. *Nature* **372**, 366-369.

Ma, D. and Jan, L. Y. (2002). ER transport signals and trafficking of potassium channels and receptors. *Curr. Opin. Neurobiol.* **12**, 287-292.

Ma, D., Zerangue, N., Lin, Y. F., Collins, A., Yu, M., Jan, Y. N. and Jan, L. Y. (2001). Role of ER export signals in controlling surface potassium channel numbers. *Science* **291**, 316-319.

Madrid, R., le Maout, S., Barrault, M. B., Janvier, K., Benichou, S. and Merot, J. (2001). Polarized trafficking and surface expression of the AQP4 water channel are coordinated by serial and regulated interactions with different clathrin-adaptor complexes. *EMBO J.* **20**, 7008-7021.

Nichols, C. G. and Lopatin, A. N. (1997). Inward rectifier potassium channels. *Annu. Rev. Physiol.* **59**, 171-191.

Nishida, M. and MacKinnon, R. (2002). Structural basis of inward rectification: cytoplasmic pore of the G protein-gated inward rectifier GIRK1 at 1.8 A resolution. *Cell* **111**, 957-965.

Nishimura, N., Plutner, H., Hahn, K. and Balch, W. E. (2002). The delta subunit of AP-3 is required for efficient transport of VSV-G from the trans-Golgi network to the cell surface. *Proc. Natl. Acad. Sci. USA* **99**, 6755-6760.

Ohno, H., Stewart, J., Fournier, M. C., Bosshart, H., Rhee, I., Miyatake, S., Saito, T., Gallusser, A., Kirchhausen, T. and Bonifacino, J. S. (1995). Interaction of tyrosine-based sorting signals with clathrin-associated proteins. *Science* **269**, 1872-1875.

Ohno, H., Fournier, M. C., Poy, G. and Bonifacino, J. S. (1996). Structural determinants of interaction of tyrosine-based sorting signals with the adaptor medium chains. *J. Biol. Chem.* **271**, 29009-29015.

Ohno, H., Aguilar, R. C., Yeh, D., Taura, D., Saito, T. and Bonifacino, J. S. (1998). The medium subunits of adaptor complexes recognize distinct but overlapping sets of tyrosine-based sorting signals. *J. Biol. Chem.* **273**, 25915-25921.

Ohno, H., Tomemori, T., Nakatsu, F., Okazaki, Y., Aguilar, R. C., Foelsch, H., Mellman, I., Saito, T., Shirasawa, T. and Bonifacino, J. S. (1999). Mu1B, a novel adaptor medium chain expressed in polarized epithelial cells. *FEBS Lett.* **449**, 215-220.

Owen, D. J. and Evans, P. R. (1998). A structural explanation for the recognition of tyrosine-based endocytotic signals. *Science* **282**, 1327-1332.

Owen, D. J., Setiadi, H., Evans, P. R., McEver, R. P. and Green, S. A. (2001). A third specificity-determining site in mu 2 adaptin for sequences upstream of YxxΦ sorting motifs. *Traffic* **2**, 105-110.

Plaster, N. M., Tawil, R., Tristani-Firouzi, M., Canun, S., Bendahhou, S., Tsunoda, A., Donaldson, M. R., Iannaccone, S. T., Brunt, E., Barohn, R. et al. (2001). Mutations in Kir2.1 cause the developmental and episodic electrical phenotypes of Andersen's syndrome. *Cell* **105**, 511-519.

Preisig-Müller, R., Schlichthorl, G., Goerge, T., Heinen, S., Bruggemann, A., Rajan, S., Derst, C., Veh, R. W. and Daut, J. (2002). Heteromerization of Kir2.x potassium channels contributes to the phenotype of Andersen's syndrome. *Proc. Natl. Acad. Sci. USA* **99**, 7774-7779.

Robinson, M. S. and Bonifacino, J. S. (2001). Adaptor-related proteins. *Curr. Opin. Cell Biol.* **13**, 444-453.

Rohde, G., Wenzel, D. and Haucke, V. (2002). A phosphatidylinositol (4,5)-bisphosphate binding site within mu2-adaptin regulates clathrin-mediated endocytosis. *J. Cell Biol.* **158**, 209-214.

Schaefer, A. W., Kamei, Y., Kamiguchi, H., Wong, E. V., Rapoport, I., Kirchhausen, T., Beach, C. M., Landreth, G., Lemmon, S. K. and Lemmon, V. (2002). L1 endocytosis is controlled by a phosphorylation-dephosphorylation cycle stimulated by outside-in signaling by L1. *J. Cell Biol.* **157**, 1223-1232.

Schram, G., Melnyk, P., Pourrier, M., Wang, Z. and Nattel, S. (2002).

Kir2.4 and Kir2.1 K(+) channel subunits co-assemble: a potential new contributor to inward rectifier current heterogeneity. *J. Physiol.* **544**, 337-349.

Shikano, S. and Li, M. (2003). Membrane receptor trafficking: evidence of proximal and distal zones conferred by two independent endoplasmic reticulum localization signals. *Proc. Natl. Acad. Sci. USA*. **100**, 5783-5788.

Simmen, T., Honing, S., Icking, A., Tikkanen, R. and Hunziker, W. (2002). AP-4 binds basolateral signals and participates in basolateral sorting in epithelial MDCK cells. *Nat. Cell Biol.* **4**, 154-159.

Stockklausner, C. and Klöcker, N. (2003). Surface expression of inward rectifier potassium channels is controlled by selective Golgi export. *J. Biol. Chem.* **278**, 17000-17005.

Stockklausner, C., Ludwig, J., Ruppersberg, J. P. and Klöcker, N. (2001). A sequence motif responsible for ER export and surface expression of Kir2.0 inward rectifier K$^+$ channels. *FEBS Lett.* **493**, 129-133.

Töpert, C., Döring, F., Wischmeyer, E., Karschin, C., Brockhaus, J., Ballanyi, K., Derst, C. and Karschin, A. (1998). Kir2.4: a novel K$^+$ inward rectifier channel associated with motoneurons of cranial nerve nuclei. *J. Neurosci.* **18**, 4096-4105.